

Article

Experimental Investigation of a Three-Bed Adsorption Refrigeration Chiller Employing an Advanced Mass Recovery Cycle

Aep Saepul Uyun ^{1,*}, Takahiko Miyazaki ², Yuki Ueda ² and Atsushi Akisawa ²

¹ Graduate School of Bio-Applications and Systems Engineering, Tokyo University of Agriculture and Technology, 2-24-16 Naka-cho, Koganei-shi, 184-8588, Tokyo, Japan

² Institute of Symbiotic Science and Technology, Tokyo University of Agriculture and Technology, 2-24-16 Naka-cho, Koganei-shi, 184-8588, Tokyo, Japan; E-Mails: tmiyazak@cc.tuat.ac.jp (T.M.); uedayuki@cc.tuat.ac.jp (Y.U.); akisawa@cc.tuat.ac.jp (A.A)

* Author to whom correspondence should be addressed; E-Mail: aepsuyun@gmail.com; asuyun@cc.tuat.ac.jp; Tel.: +81-42-388-7282

Received: 8 June 2009; in revised form: 13 July 2009 / Accepted: 16 July 2009 /

Published: 17 July 2009

Abstract: The performance of an advanced three-bed adsorption chiller with a mass recovery cycle has been experimentally investigated in the present study. The temperature and pressure of various components of the chiller were monitored to observe the dynamic behaviour of the chiller. The performances in terms of the coefficient of performance (COP) and specific cooling power (SCP) were compared with a conventional single stage. The results show that the proposed cycle produces COP and SCP values superior to those of the conventional single stage cycle for heat source temperature below 75 °C.

Keywords: adsorption chiller; performance; mass recovery; low temperature heat source

1. Introduction

Adsorption chillers are usually driven by heat, so these chillers are attractive for reducing electric power demand peaks resulting from air-conditioning and refrigeration equipment loads. The variety of heat sources available for driving the adsorption refrigeration cycle makes this a technology that

contributes to CO₂ reduction by utilizing non-fossil fuel, such as solar energy or waste heat from industrial process, as its driving source [1]. It has been reported that the fixed beds of porous materials in the adsorption refrigeration cycles tend to be low performance, long cycle time and make the system over-sized due to poor heat and mass transfer rates in the adsorption bed [2].

Most of the research in this field focuses on developing advanced cycles in order to improve chiller performance to be competitive with other systems. Silica gel–water is widely used as an adsorbent–adsorbate pair in adsorption refrigeration system. Compared to other adsorbents, silica gel can be regenerated at a relatively low temperature that is below 100 °C. It also has a large uptake capacity for adsorption of water up to 35–40% of its dry mass, which has a high latent heat of evaporation. Because of the low regeneration temperature, a silica gel–water adsorption chiller can utilize industrial waste heat or renewable energy resources [3–5].

The intensive research on developing silica gel–water adsorption chiller has been done by many researchers. For example, the multi-bed multi-stage cycle is able to produce a cooling effect at low heat source temperature such as below 100 °C. To utilize the low heat source temperature, a three-stage silica gel–water adsorption cycle was proposed and examined by Saha *et al.* [6]. In a similar effort, these authors [7] introduced a two-stage chiller and the driving heat source temperature was experimentally validated. The cycles have ability to drive the chiller with a low heat source temperature; however, they have a lower coefficient of performance (COP) [8].

The performance of the adsorption refrigeration cycle can be enhanced by applying a mass recovery cycle into the adsorption cycle [9–11]. The mass recovery cycle is produced by interconnecting the two beds for depressurizing and pressurizing after desorption and adsorption processes, respectively. Conceptually, the pressure difference between two beds in the beginning of the process will causes refrigerant flows until a pressure balance is reached between the beds. Akahira *et al.* [9,10] determined that the mass recovery cycle provides heating to the desorber and cooling to the adsorber. They reported that the cycle produces better performance than that of conventional mass recovery without heating and cooling. The mass recovery cycle can also be applied to multi-bed and multi-stage cycles. Alam *et al.* [8] introduced the mass recovery cycle into a two-stage adsorption cycle, namely, a re-heat two-stage adsorption cycle. A similar effort was also made by Khan *et al.* [12], applying the scheme to a three-stage adsorption cycle. They reported that the cycle produces a higher COP value than those of conventional two-stage and three-stage cycles. The advanced mass recovery cycle was also applied to a three-bed cycle. Khan *et al.* [13] proposed and numerically evaluated a three-bed mass recovery cycle. They reported that the cycle performance is better than that of the three-bed single stage proposed by Saha *et al.* [14]. Uyun *et al.* [15] proposed and investigated numerically the advanced three-bed adsorption cycle employing heat and mass recovery cycle. They obtained that the performance of the cycle are superior to those of three-bed of single stage and mass recovery cycle.

As improvement upon the conventional single stage adsorption cycle, this paper experimentally investigates the performance of a three-bed cycle employing an advanced mass recovery cycle [15]. It should be noted that the mass recovery mechanism of the proposed cycle is rather different from the conventional system. The proposed cycle combines a single stage and a mass recovery cycle into one cycle. The beds can be divided into two cycles with different working pressures of the refrigerant release mechanism. The two beds, namely, high adsorber 1 (HA₁) and high adsorber 2 (HA₂), work at the high pressure of condenser in the desorption-condensation process, while another bed, namely, low

adsorber (LA), works at the middle pressure of the mass recovery mechanism. Both HA_1 and HA_2 function as the main compressor of the cycles. Similarly, LA functions as the intermediate bed that bridges the pressure and concentration gap of the cycle. To reach the condenser pressure, the LA must undergo two pressurization steps. This is almost identical to the two-stage cycle. However, in the mass recovery process, the refrigerant transfer begins at the same concentration level.

Further explanation of the cycle principle is given in the Working Principle section. The temperature and pressure of each heat exchanger component will be discussed in detail to determine the dynamic behavior of the cycle. In order to evaluate the improvement in performance, a comparison with conventional single stage adsorption refrigeration cycle will also be presented in terms of specific cooling power and the coefficient of performance.

2. Working Principle

The adsorption cycle consists of a three-bed adsorber containing silica gel, namely high adsorber 1 (HA_1), high adsorber 2 (HA_2) and low adsorber (LA). The processes in the cycle can be divided into eight modes. The processes that occur in each adsorbent can be explained as follows (Table 1a). In mode A, HA_1 is in the heating process, while LA and HA_2 are in the cooling process. The heating system provides heat to HA_1 for the desorption process. This process provides sufficient energy for releasing the refrigerant from adsorbent pores, and the refrigerant then vaporizes to the condenser. By opening valve Vv_3 the refrigerant vapor will flow to the condenser. In the desorption process, the resulting refrigerant is cooled down in the condenser by circulating cooling water from the cooling system, which removes condensation heat. The desorption-condensation process occurs at condenser pressure (P_{cond}), as shown in Figure 2, path 1–2. After the condensation process, liquid refrigerant flows to the evaporator. The evaporator is connected to HA_2 and LA by opening valves Vv_7 and Vv_4 , respectively. In the adsorption-evaporation process, the refrigerant in the evaporator is evaporated at a low temperature (T_{eva}) and captures heat (Q_{eva}) from chilled water. The evaporated vapor is adsorbed by HA_2 and LA. The cooling system also supplies cooling water to HA_2 and LA to remove adsorption heat released during the adsorption process. The adsorption-evaporation process occurs at evaporation pressure (P_{eva}). The process can be seen in Figure 2 at paths 3–4 and 9–6 for HA_2 and LA, respectively.

In mode B, HA_2 continues the adsorption-evaporation process by remaining connected to the evaporator as described in mode A. Meanwhile, HA_1 and LA are now involved in the pre-cooling and pre-heating processes, respectively. HA_1 and LA are isolated from the other heat exchanger by closing valves Vv_1 , Vv_2 , Vv_3 , Vv_4 and Vv_5 . As can be seen in Figure 2, at the end of the desorption process (mode A), the pressure of HA_1 is at the high condenser pressure. Therefore, to switch the stage from desorption to the adsorption process, the pressure of HA_1 should be reduced to the evaporator pressure, which can be done by reducing temperature. The cooling water from the cooling tower is flowed to HA_1 . Consequently, the temperature as well as the pressure of HA_1 decreases from point 2 to point 3. In contrast to HA_1 , in mode B, the LA is in the pre-heating process (6–7). The objective of this process is to increase the pressure of LA before the mass recovery process begins in mode C. The initial pressure difference between LA and HA_2 is required at the start of the mass recovery process to make it effective. During the mass recovery process, LA is still in the heating process to achieve additional force for releasing the refrigerant. At the same time, HA_2 continues the cooling process. In other words,

LA and HA₂ are in mass recovery while undergoing heating and cooling processes, respectively. The processes can be seen in Figure 2, path 7–8 and path 4–5 for LA and HA₂, respectively. Concurrently, the cooling process occurs at HA₂ for effectively adsorbing refrigerant vapor.

Table 1. Chiller heat exchanger state.

a. The proposed cycle

Bed	Mode							
	A 270 s	B 60 s	C 240 s	D 30 s	E 270 s	F 60 s	G 240 s	H 30 s
HA ₁	Des	Pc	Ads				Mc	Ph
LA	Ads	Ph	Mh	Pc	Ads	Ph	Mh	Pc
HA ₂	Ads		Mc	Ph	Des	Pc	Ads	

b. The single stage cycle

Bed	Mode			
	A 540 s	B 60 s	C 540 s	D 60 s
HA ₁	Des	Pc	Ads	Ph
LA	Ads	Ph	Des	Pc
HA ₂	Ads	Ph	Des	Pc

- Des : Desorption process
 - Ph : Pre-heating process
 - Mh : Mass recovery heating
 - Ads : Adsorption process
 - Pc : Pre-cooling process
 - Mc : Mass recovery cooling
- Heating process
 Cooling process

In mode C, HA₁ acts as an adsorber and is connected to the evaporator to start the mode. The process is identical to the adsorption-evaporation process that occurs in HA₂ (mode A). In mode D, LA and HA₂ are in pre-cooling (8–9) and pre-heating processes (5–1), respectively. In this mode, LA is cooled by cooling water and HA₂ is heated by hot water. This mode is the initial condition for LA and HA₂ before the adsorption and desorption process begin in mode E. In modes E–H, the process occurring in LA is similar to the corresponding process modes A–D. The difference is that HA₁ and

HA₂ are in interchanged positions. For instance, in mode E, LA is in the same process, adsorption, as in mode A. However, the positions of HA₁ and HA₂ are reversed from mode A.

Figure 1. Schematic diagram of three-bed adsorption refrigeration cycle.

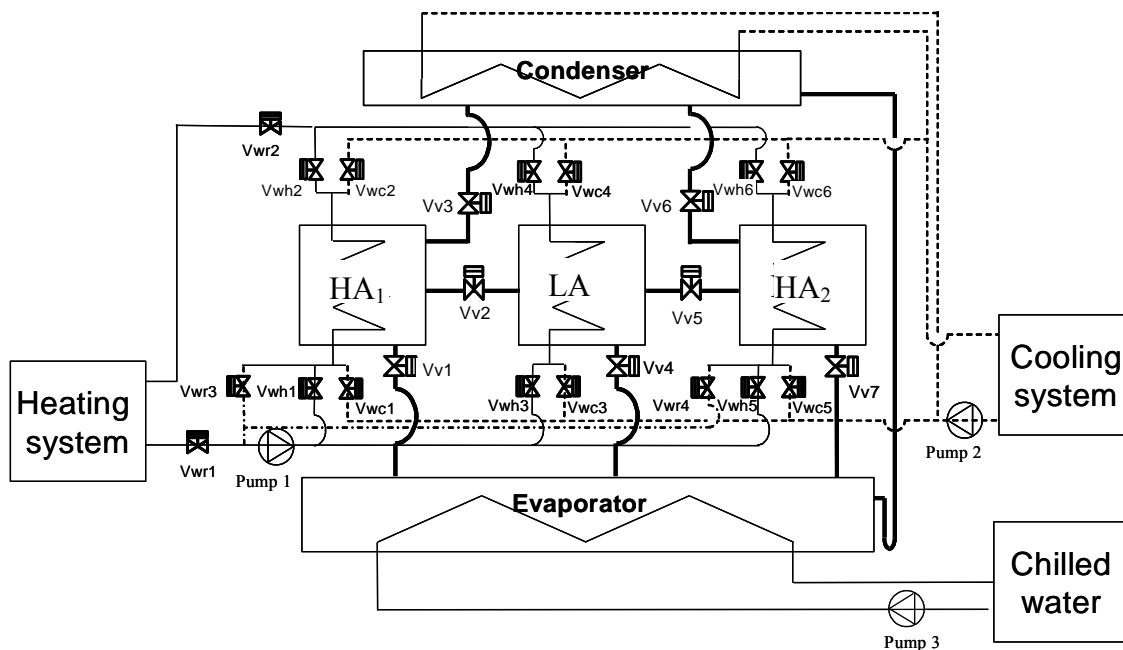
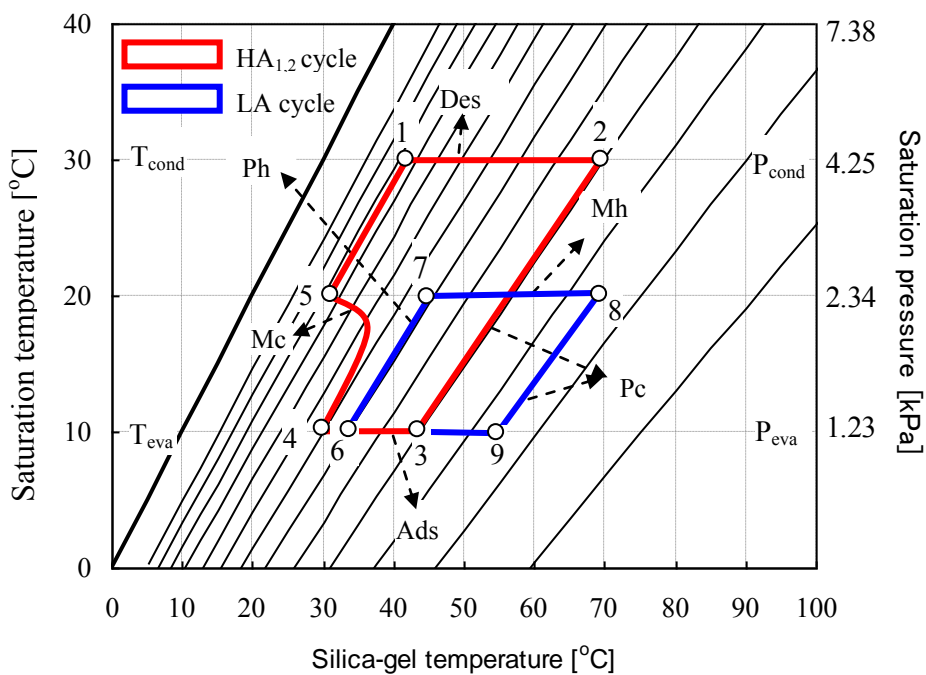


Figure 2. Theoretical of the proposed cycle on P-T-X diagram.



The working principle of the conventional single stage is presented in Table 1b. The conventional single stage cycle requires at least two-bed adsorber to obtain a continuous refrigeration cycle. Since the performance of the cycles is influenced by the total mass of adsorbers, the total adsorber should be

identical for both the single stage and the proposed cycle. In the present study, the LA and HA₂ combine into one bed and perform the same mode. It can be seen in the table that mode A of the single stage cycle is similar to modes A and E of the proposed cycle, where one bed of HA performs the desorption process while another bed of combined HA and LA performs the adsorption process. Further explanation of the cycle and allocation time in each mode is shown in the Table 1.

3. Experiment Apparatus and Measurement

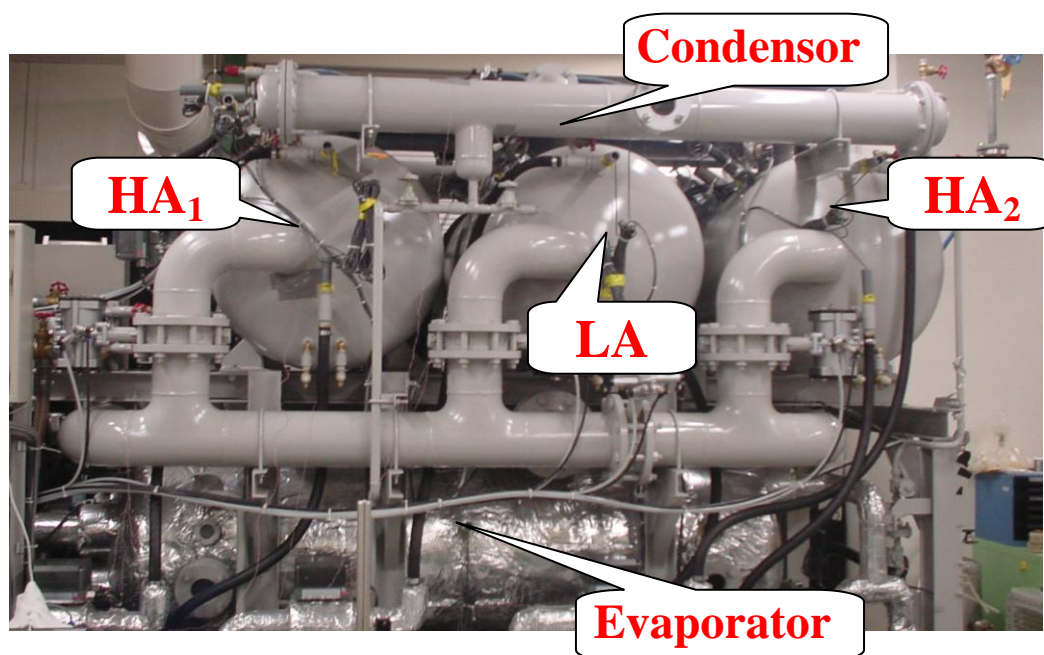
3.1. Experimental apparatus description

Figure 3 shows a photograph of the experimental adsorption chiller. The experimental chiller has six adsorption/desorption beds, two condensers, and two evaporators. It is designed to test various operation modes of adsorption cycles. Though the chiller has six adsorbent heat exchangers, only a three-bed heat exchanger is required for the present cycle. The experimental chiller also consists of three types of reservoir tanks installed outside the room, namely, a hot water tank, a cooling water tank, and a chilled water tank.

Three heaters installed in the heating water tank can be controlled automatically or manually by switching the boiler on or off. A pump is used to circulate heating water in the experimental chiller. The heater is also installed in the chilled water tank to fix the inlet chilled water temperature. It works automatically when the inlet chilled water temperature is lower than the set chilled water inlet value.

Cooling water flows to adsorber and the condenser and is then mixed in the outlet cooling pipe before being pumped to the cooling water tank. A cooling tower installed in the cooling water tank decreases the heat to an ambient temperature. A water pump is used to circulate cooling water back into the chiller.

Figure 3. Photograph of the experimental device.



3.2. Experimental procedure

Three kinds of measurements were performed in the experiment: temperature, pressure and mass flow rate. In the beds, the thermistors Pt100 Ω (± 0.2 °C) were used to measure temperatures of beds, of refrigerant vapor and of inlet and outlet water. The same thermistors Pt100 Ω (± 0.2 °C) were used in condensers and evaporators to measure the temperatures of the inlet and outlet water of the cooling condensers and the chilled water inlet and outlet. Pressure sensors (± 0.125 kPa) were used to measure the pressures of the beds the condenser, and the evaporator. Electromagnetic flow meters ($\pm 0.2\%$) were used to measure the flow rate of the cooling water and heating water, the flow rate of the cooling water into the condenser and the flow rate of the chilled water into the evaporator. It is estimated that the accuracy of the heat input measurements is $\pm 2.4\%$, average cooling power is $\pm 2.9\%$ and COP measurements is $\pm 5.5\%$.

The water flow rate setups were changed by manually-operated valves, and the adsorption-desorption cycle times were adjusted via a control panel to input new cycle time values into the chiller's built-in control software. Tests were firstly done for the standard conditions shown in Table 2. All sensors were connected to a data logger and collected every second. The data measurements were taken after a cycle steady state had been reached. A micro-computer was used to collect and process the measurement data.

Table 2. Standard operating conditions.

Parameter		Value	Unit
Hot water in	Temp	70	°C
	Flow	0.53	kg/s
Cooling water in	Temp	14	°C
	Flow	0.98	kg/s
	(ads+cond)	0.53+0.45	
Chilled water in	Temp	14	°C
	Flow	0.2	kg/s
Cycle time		1200	s
Desorption time		270	s
Mass recovery time		240	s
Pre-heating time	HA _{1,2}	30	s
	LA	60	s
Pre-cooling time	HA _{1,2}	60	s
	LA	30	s

4. Performance Indicators

The Coefficient of Performance (COP) and Specific Cooling Power (SCP) are two performance value indicators used to evaluate cycle performance. The COP value shows the system efficiency and

is defined as the ratio between chilled water power (Q_{chill}) and heat input (Q_{in}) into the system. The average heat input to the system can be estimated as:

$$Q_{in} = \frac{F_{hot} C_w}{t_{cycle}} \int_0^{t_{cycle}} (T_{hot,in} - T_{hot,out}) dt \quad (1)$$

and the average chilled water power (cooling capacity) as:

$$Q_{chill} = \frac{F_{chill} C_w}{t_{cycle}} \int_0^{t_{cycle}} (T_{chill,in} - T_{chill,out}) dt \quad (2)$$

Therefore, the COP can be written as:

$$COP = \frac{Q_{chill}}{Q_{in}} \quad (3)$$

The SCP value indicates the chiller's capacity to produce a cooling effect in relation to the total mass of the adsorbent used. The SCP value can be expressed as:

$$SCP = \frac{Q_{chill}}{M_{tot}} \quad (4)$$

where F_{hot} , F_{chill} , T_{hot} , and T_{chill} are the hot water mass flow rate, chilled water mass flow rate, hot water temperature, and chilled water temperature, respectively. C_w and M_{tot} denote the water isobaric specific heat (4180 J/kg K) and total silica gel mass (16 kg per bed), respectively. T_{cycle} and dt are cycle time and interval time (s), respectively. The suffixes in and out refer to inlet and outlet of water flow.

5. Results and Discussion

The experiments were conducted to test the performance of a three-bed adsorption cycle. In the beginning of the experiment, the chiller condition was not balanced. However, after several cycles, the chiller reached its cyclic steady state, as indicated by all inlet temperatures being at the desired levels.

5.1. Temperature and pressure behaviors

Figures 4 and 5 show the temperature and pressure behaviors of the beds when the heat source temperature was 70 °C, and the cycle time is as shown in Table 2. In mode A, HA₁ and LA are in the desorption and adsorption processes, respectively. The temperature and pressure of HA₁ increase because hot water is supplied to the bed for providing heat during the desorption process. At the same time, the temperatures of LA decrease because cooling water from the cooling tower is flowed to those beds for removing bed heat during the adsorption process. Mode E is identical to mode A. However, the position of HA₂ is interchanged with the position of HA₁, where HA₁ and HA₂ are in the adsorption and desorption processes, respectively. For the mass recovery process (mode C and mode G) in the beginning, the temperature of LA decreases while HA₂ (mode C) or HA₁ (mode G) increases,

even though LA and HA_{1,2} are in heating and cooling modes, respectively (see point 1, Figure 4). When HA_{1,2} and LA are connected to each other, the saturation pressure of the beds suddenly changes, causing LA to begin desorption and LA to rapidly begin adsorption of water vapor. Therefore, for several seconds the temperature of LA decreases and that of HA_{1,2} increases. Subsequently, the temperature of LA begins to increase and that of HA_{1,2} to decrease.

Figure 4 shows the temperature profile difference during the heating process of HA_{1,2} (desorption process) and LA (mass recovery process). It can be seen that the maximum temperature of HA_{1,2} (point 2) is lower than that of LA (point 3). The lower temperature of HA_{1,2} denotes high energy consumption compared to that of LA. As explained in the Working Principle section, HA_{1,2} functions as the main compressor that bridges the refrigerant flow from LA to the condenser. In addition to acting as an adsorber during the adsorption-evaporation process, HA_{1,2} also adsorbs and collects the refrigerant from LA during the mass recovery process. Therefore, the total refrigerant amount of HA_{1,2} that should be released during desorption process is higher than the total refrigerant amount of LA that should be released during the mass recovery process. The other reason for the maximum temperature difference is the difference in working pressures. Figure 5 shows that the desorption process occurs at the high pressure of the condenser, while mass recovery works at the medium pressure of mass recovery. The initial difference in pressures between the two beds in the mass recovery process provides a greater bed driving force for releasing the refrigerant. In other words, because of the amount of total refrigerant released, as well as the high pressure of HA_{1,2}, the heat input during the desorption process of HA_{1,2} is higher than that for the mass recovery process.

Figure 4. Temperature histories of adsorbent beds, condenser (T_c), and evaporator (T_e) of the proposed cycle.

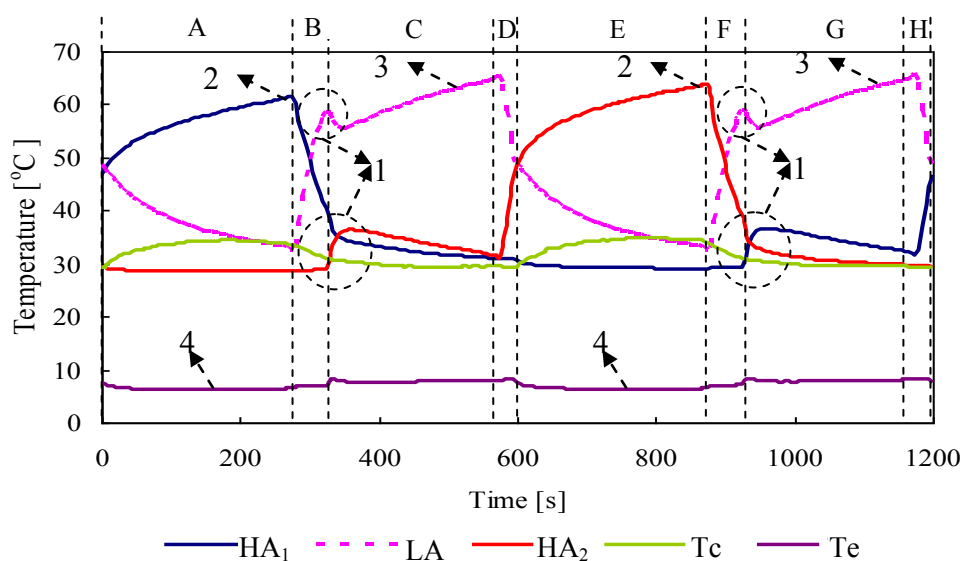


Figure 4 also shows that in mode A and E, the temperature of the evaporator is lower than in other modes. This can be understood because in those modes LA and HA₁ (mode A) or HA₂ (mode E) are connected to the evaporator for the adsorption-evaporation process. Therefore, the evaporator temperature will decrease more sharply compared to the modes in which only HA₁ or HA₂ is connected to the evaporator (see point 4, Figure 4).

Figure 5. Pressure histories of the proposed cycle.

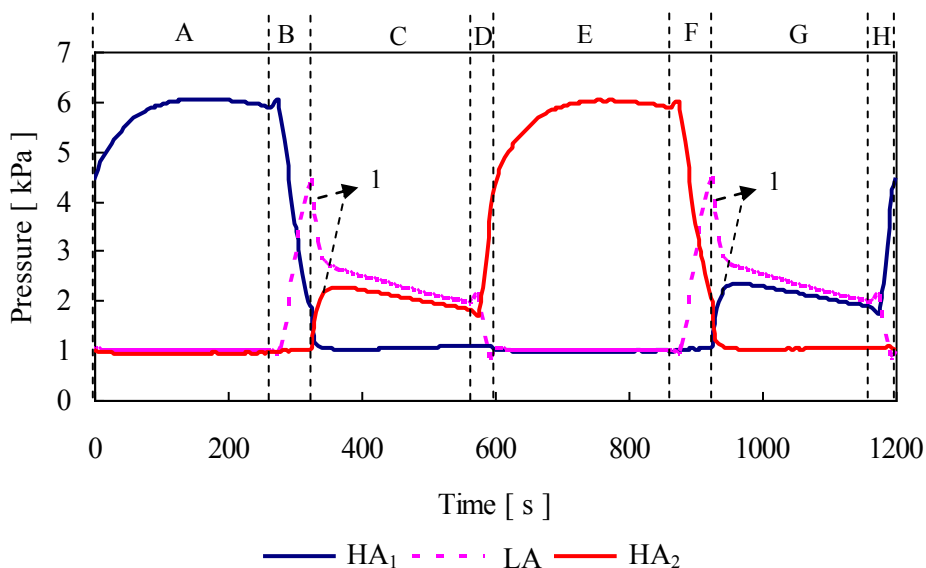


Figure 6 shows the Duhring diagram (PTX diagram) of the cycle, which describes the detail of adsorption behavior in one refrigeration cycle. It can be seen that the profile diagrams of each bed resemble the ideal cycle. It can also be seen that the pressure of the desorption process in the experimental results is higher than that of the ideal process. It is caused by the vapor flowing to condenser, which is higher than the condensation rate of condenser. In other words, it requires condenser which has high capacity in releasing condensation heat to get optimum condensation process.

It can also be observed from Figure 6 that in the present observation of the mass recovery process, the maximum concentration of HA adsorbers cannot be achieved. The HA adsorbers do not optimally adsorb refrigerant released from LA. This may indicate that more heat rejection of mass recovery cooling is needed for this process to reach maximum concentration of refrigerant adsorbed as shown by an ideal cycle.

Figure 6. PTX diagram of the experimental result (heat source temperature is 70 °C).

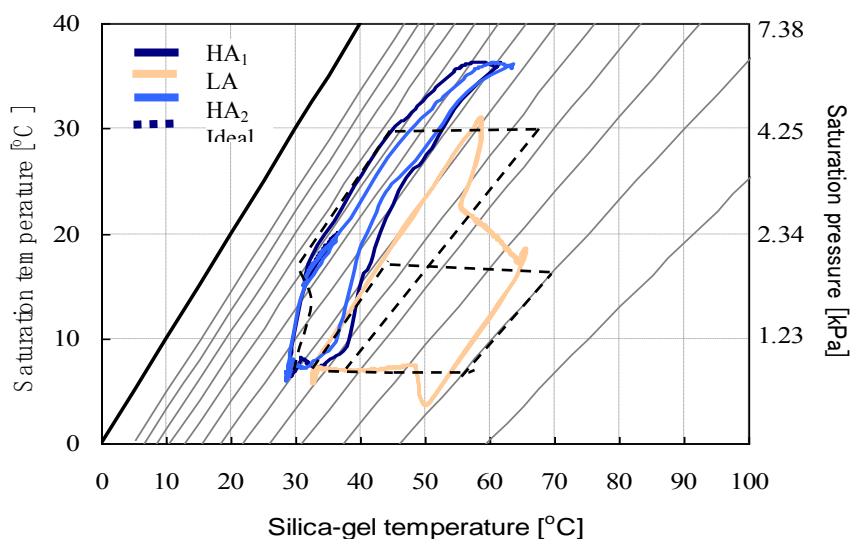
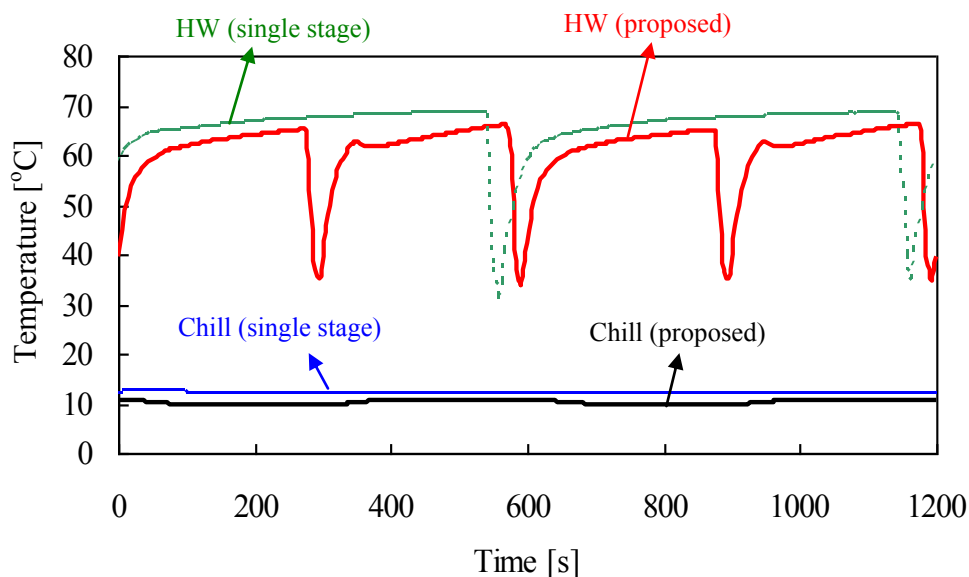


Figure 7. Hot water (HW) and chilled water (Chill) outlets of the proposed cycle and the conventional single stage cycle.



5.2. Comparison with conventional single stage cycle

Figures 7–10 show the comparison of the experimental results between the proposed cycle and the conventional cycle. Both of the cycles were tested at the same conditions based on the input parameters presented in Table 2. Figure 7 shows the comparison of the hot and chilled water outlets of the proposed cycle and conventional single stage cycle. It shows that the temperatures of the hot and chilled water outlets of the proposed cycle are lower than the corresponding outlets of the single stage. The low temperatures of the hot water outlet indicate that the cycle consumes more energy compared to the conventional single stage, as presented in Figure 8. It is clearly shown in that figure that if the heat source temperature is at 70 °C, the proposed cycle requires by 53% more heat input than the single stage. However, the proposed cycle produces a high cooling capacity. The cooling capacity can be improved more than 80% using the proposed cycle, as well as increasing the SCP from that of conventional cycle.

Figure 9 shows the comparison of the proposed cycle and the single stage cycle in terms of COP and SCP values in the range of heat source temperature from 65 to 80 °C. The advantage of COP for low temperature of the heat source means that LA cycle works dominantly in that range. In contrast, contribution of LA cycle becomes smaller when the heat source temperature is higher. This is a reason why the difference of COP between the two cycles reduces as heat source temperature increases. From the figure, it is clearly found that COP of the proposed cycle is higher than that of the single stage if heat source temperature is below 75 °C. It should be noted that performance of the propose cycle is much better than that of the single stage cycle although COP are almost the same at a heat source temperature of 80 °C. This is because the chilled water outlet temperature of the single stage cycle is higher than that of the proposed cycle as shown in Figure 10.

Figure 8. Comparison of the proposed cycle and the conventional single stage cycle on average heat input (Q_{in}) and cooling capacity (CC).

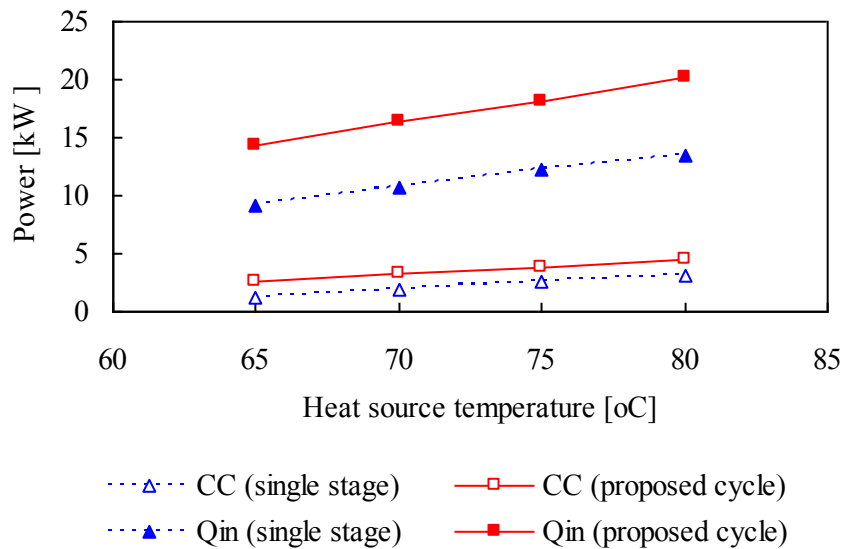
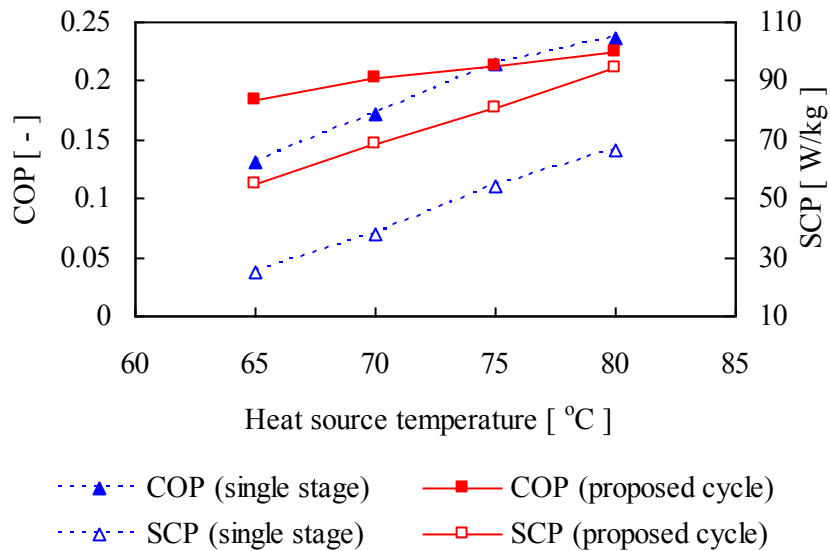


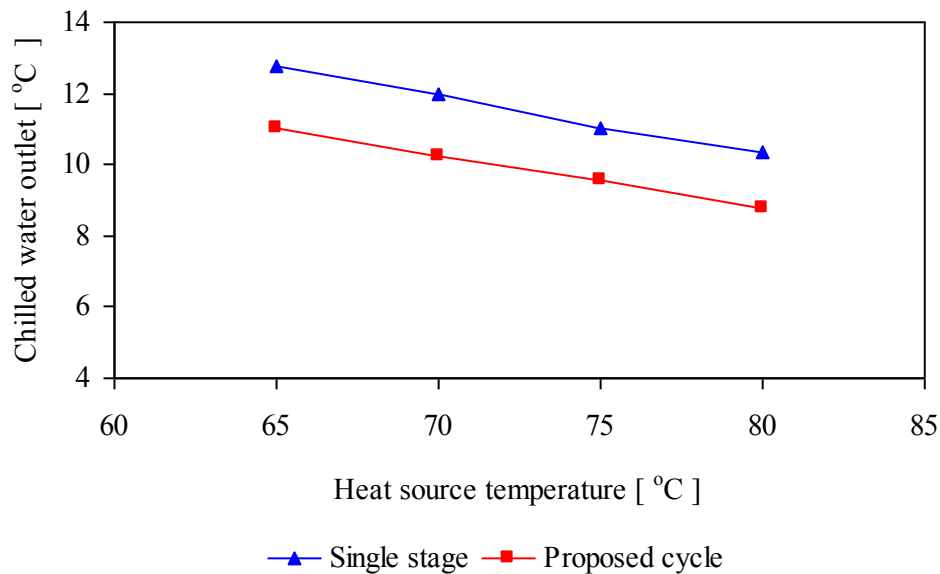
Figure 9. Performance comparison of the proposed cycle and the conventional single stage cycle in terms of COP and SCP.



The ability to produce a low chilled water outlet is one of the indicators to test the performance of the new cycle. According to Figure 10, the proposed cycle is able to produce chilled water at lower temperature than that of the single stage. It is considered practically impossible for the single stage cycle to generate such a cooling effect as the proposed cycle does at such low heat source temperature below 70 °C . The cycle mode allocation of the proposed cycle allows for the production of a cooling effect, as well as cold chilled water, in each mode. According to Table 1, two beds are connected to the evaporator in modes A and E. Likewise, one bed of HA is connected to the evaporator in the other mode for the adsorption-desorption process. Thus, in every mode of the cycle, at least one bed is connected to the evaporator, which produces a cooling effect continuously. It also can be seen from Table 1 that one cycle of the desorption-adsorption process consists of four smaller cycles. These are

two cycles for LA and one cycle for each of the HA. In other words, although the proposed cycle uses only three beds of adsorbents, it can produce four cycles similar to a four-bed adsorption cycle.

Figure 10. Performance comparison of outlet chilled water between the proposed cycle and the conventional single stage cycle.



6. Conclusions

The performance of a three-bed adsorption chiller applying a new mass recovery cycle scheme was investigated experimentally. In the investigation of the dynamic behavior of the cycle, it can be concluded that one completed cycle of the proposed cycle consists of four cycles. That is similar to the number of cycles produced by a conventional four-bed adsorption cycle. However, the proposed cycle requires only three adsorber beds, which suggests it can be more compact than conventional four-bed adsorption cycle.

In comparison to the single stage cycle, the chiller performance of the proposed cycle is higher compared to the conventional cycle in terms of the SCP and COP values, especially for heat source temperatures below 75 °C. The chiller also allows production of outlet chilled water of lower temperature for all heat source temperatures observed.

References and Notes

1. Ng, K.C.; Wang, X.; Lim, Y.S.; Saha, B.B.; Chakarborty, A.; Koyama, S.; Akisawa, A.; Kashiwagi, T. Experimental study on performance improvement of a four-bed adsorption chiller by using heat and mass recovery. *Int. J. Heat Mass Transfer* **2006**, *49*, 3343–3348.
2. Qu, T.F.; Wang, R.Z.; Wang, W. Study on heat and mass recovery in adsorption refrigeration cycles. *Appl. Therm. Eng.* **2001**, *21*, 439–452.
3. Chua, H.T.; Ng, K.C.; Wang, W.; Yap, C.; Wang, X.L. Transient modeling of a two-bed silica gel-water adsorption chiller. *Int. J. Heat Mass Transfer* **2004**, *47*, 659–669.

4. Saha, B.B.; Koyama, S.; Kashiwagi, T.; Akisawa, A.; Ng, K.C.; Chua, H.T. Waste heat driven dual-mode, multi-stage, multi-bed regenerative adsorption system. *Int. J. Refrig.* **2003**, *26*, 749–757.
5. Ng, K.C.; Chua, H.T.; Chung, C.Y.; Loke, C.Y.; Kashiwagi, T.; Akisawa, T.; Saha, B.B. Experimental investigation of the silica gel-water adsorption isotherm characteristics. *Appl. Therm. Eng.* **2001**, *21*, 1631–1642.
6. Saha, B.B.; Boelman, E.C.; Kashiwagi, T. Computational analysis of an advanced adsorption-refrigeration cycle. *Energy* **1995**, *20*, 983–994.
7. Saha, B.B.; Akisawa, A.; Kashiwagi, T. Solar/waste heat driven two-stage adsorption chiller: the prototype. *Renewable Energy* **2001**, *23*, 93–101.
8. Alam, K.; Khan M.; Uyun, A.S.; Hamamoto, Y.; Akisawa, A.; Kashiwagi, T. Experimental study of a low temperature heat driven re-heat two-stage adsorption chiller. *Appl. Therm. Eng.* **2007**, *27*, 1686–1692.
9. Akahira, A.; Alam, K.C.A.; Hamamoto, Y.; Akisawa, A.; Kashiwagi, T. Experimental investigation of mass recovery adsorption refrigeration cycle. *Int. J. Refrig.* **2005**, *28*, 565–572.
10. Akahira, A.; Alam K.C.A.; Hamamoto, Y.; Akisawa, A.; Kashiwagi, T. Mass recovery four-bed adsorption refrigeration cycle with energy cascading. *Appl. Therm. Eng.* **2005**, *25*, 1764–1778.
11. Alam, K.C.A.; Akahira, A.; Hamamoto, Y.; Akisawa, A.; Kashiwagi, T. A four-bed mass recovery adsorption refrigeration cycle driven by low temperature waste/renewable heat source. *Renewable Energy* **2004**, *29*, 1461–1475.
12. Khan, M.Z.I.; Alam, K.C.A.; Saha, B.; Akisawa, A.; Kashiwagi T. Performance evaluation of multi-stage, multi-bed adsorption chiller employing re-heat scheme. *Renewable Energy* **2008**, *33*, 88–98.
13. Khan, M.Z.I.; Saha, B.B.; Alam, K.C.A.; Akisawa, A.; Kashiwagi, T. Study on solar/waste heat driven multi-bed adsorption chiller with mass recovery. *Renewable Energy* **2007**, *32*, 365–381.
14. Saha, B.B.; Koyama, S.; Lee, J.B.; Kuwahara, K.; Alam, K.C.A.; Hamamoto, Y.; Akisawa, A.; Kashiwagi, T. Performance evaluation of a low-temperature waste heat driven multi-bed adsorption chiller. *Int. J. Multiphase Flow* **2003**, *29*, 1249–1263.
15. Uyun, A.S.; Akisawa, A.; Miyazaki, T.; Ueda, Y.; Kashiwagi, T. Numerical analysis of an advanced three-bed mass recovery adsorption refrigeration cycle. *Appl. Therm. Eng.* DOI: 10.1016/j.applthermaleng.2009.02.008 (accessed July 17, 2009).